Electro-thermal-mechanical Performance of a sensor based on PAN Carbon Fibers and Real-Time Detection of Change Under Thermal and Mechanical Stimuli

Yumna Qureshi* [(a)], Mostapha Tarfaoui*[(a)], Khalid Lafdi[(b,c)]

(a) ENSTA Bretagne, IRDL - UMR CNRS 6027, F-29200 Brest, France.

(b) University of Dayton, Nanomaterials Laboratory, Dayton, OH 45469-0168, United States

(c) Department of Mechanical and Construction Engineering, Northumbria University, Newcastle upon Tyne, UK

Abstract: Structural health monitoring (SHM) is a vastly growing field consisting of sensors embedded in or attached with the structure which respond to the strain or other stimuli to monitor the deformation in real-time. In this study, a carbon fiber (CF) sensor was developed using unidirectional Polyacrylonitrile (PAN) carbon filaments aligned straightly together and its sensitivity was calculated experimentally, with the gauge factor (GF) in 10.2-10.8 range. The electro-thermal behavior of this CF sensor showed distinct performance and detected the change in the surrounding temperature. There is a good reproducibility in the results in both piezoresistive and electro-thermal behavior of the CF sensor and its electrical performance showed real-time detection of both mechanical and thermal stimuli. The results established that the CF exhibited good potential as a flexible strain sensor for in-situ monitoring of damage or energy release during the failure of composites.

Keywords: Real-time monitoring system, PAN carbon fiber sensor, electromechanical performance, electro-thermal behavior

---

*Corresponding author:
E-mail address: yumna.qureshi@ensta-bretagne.org, mostapha.tarfaoui@ensta-bretagne.fr
Fax: +33 2 98 34 87 30

1. Introduction

The detection of local damage such as delamination, interlaminar failure, matrix softening, and matrix cracking in composites is often difficult to detect unless the performance of the materials has been compromised [1]–[7]. Non-destructive techniques (NDT) such as ultrasonic detection, X-rays, etc. can detect local damage however they often require disassembly of the structure for inspection and they aren't able to detect damage in instantaneously. Acoustic emission is often used for real-time monitoring of the failure in structures but, interpretation of the data is a complex process and mostly qualitative. So, it is important to develop novel techniques to monitor the deformation of the structure in real-time, and structural health monitoring (SHM) is a renowned and extensively used system to study the behavior of the structure in real-time to guarantee their reliability and safety [8]–[12].

Currently used SHM techniques include fiber optic sensors, piezoelectric or piezoresistive sensors, strain gauges, and accelerometers to monitor the mechanical deformation, vibrations, or other parameters of the structure during the operation [13]–[23]. However, most of these techniques can detect damage near its location therefore they must be placed near the critical zones on the structure. To counter this, sensors network systems had also been used to triangulate the location of the damage using lamb wave propagation, but the cost, size, and weight of such a system limit their use not to mention the complex data processing required [24]. Moreover, SHM systems attached to the surface of the composites such as optical fibers and strain gauges had a drawback of being exposed to the environmental conditions, for example, chemical, thermal, humidity, and external mechanical effect [25], [26]. That is why researchers are more focused on integrable monitoring sensors to not only monitor the overall deformation of the structure but to also monitor the internal behavior between the laminates of the composites. However, the insertion of the monitoring sensor entity in the composites is still underdeveloped and the prime focus is that it would not affect the performance of the composite structures. In previous studies, various sensors were developed and inserted inside the composites such as fiber Bragg grating, carbon nanotubes, carbon black, or carbon fibers [27]–[32]. Nowadays, nanomaterials had also been used to developed highly sensitive and flexible strain sensors and tested under different loading conditions for application such as multimode skin sensors, SHM of structural components and to monitor human movement etc. [33]–[36]. However, the use of optical sensors methods is limited because of the high cost to produce an optical fiber with fiber Bragg grating. Moreover, the use of nanomaterials as a damage sensing system is quite complex and expensive.

In comparison, carbon fibers (CF) used as a sensor because of their good electrical conductivity is a possible simple, durable, and cost-effective solution for damage monitoring in real-time[37]. CF consists of graphite-based microstructure and loading these fibers could deduce change in electrical behavior because of the change in their mechanical structure thus, depicting piezoresistive

behavior[38]. Besides, the integration of CF in fiber-reinforced composites is quite easy because of the textile processing compatibility [39]ï [41]. The electromechanical response of Carbon fibers was the first study by Concor and Owston [42] which showed that resistance of these fibers rises linearly with the applied strain and they also studied their mechanical performance and contact resistance [39]. After these studies, continuous carbon fibers had been in use as self-sensing materials in composites because of simplicity in application, high mechanical performance, and less cost[43]ï [50]. However, straightness of the filaments in the CF sensor plays a vital role to define the contact resistance and overall performance of the sensor[42], [48], [49].

In this experimental investigation, the real-time monitoring ability of the CF sensor, consisting of unidirectional carbon filaments aligned together, was examined. The sensitivity of the CF to the applied strain was calculated experimentally by the gauge factor (GF) calculation using a standalone sensor. Afterwards, the general electromechanical behavior of the CF sensor was examined up to fracture to validate its response under large strain application or during any damage that was vital to comprehend its use in high strain applications. In the next step, this CF sensor was attached to the electrodes and put in an oven to monitor the change in its electrical behavior during the change in temperature of its surroundings. The results gave interesting behavior and showed that CF sensor did not only detected the strain under mechanical loading but also showed the change in its resistance under thermal loads, which could be useful in detecting the release of thermal energy in a structure because of the presence of macro or micro cracks [7].

2. Material and Experimentation

Carbon fibers (CF) consisted of unidirectional filaments of Polyacrylonitrile (PAN) carbon fibers which were purchased from the Nanomaterials Laboratory of the University of Dayton. First, PAN Fibers are thermally stabilized at 200-300°C at room temperature and then, these fibers were carbonized in an inert environment above 1000°C. Afterwards, the surface of the fibers was etched during surface treatment. Some of the physical properties are mentioned in Table 1 for the PAN carbon fibers. SEM characterization was performed to demonstrate the filaments of CF, Figure 1.

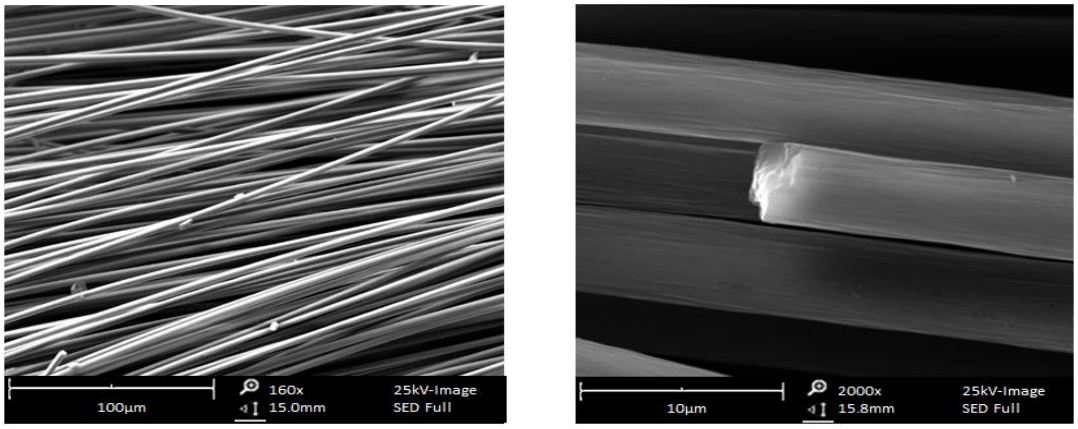

(a) *(b)*

Figure 1: SEM images of the CF sensor. (a) SEM of unidirectional filaments of Carbon aligned together (b) magnified image to show the single fiber of carbon

Table 1: Physical Properties of the PAN Carbon Fibers

Density (g/cc)	1.76
Coefficient of thermal expansion (CTE) (µm/m-°C)	-0.6
Thermal Conductivity (W/m-K)	8.50
Electrical Resistance (ohm-cm)	0.00180

2.1. Experimentation of standalone CF sensor under mechanical loading

CF sensor was tested under tensile load as a standalone sensor of 72 mm length and 5 mm width using the INSTRON-50 apparatus. The data acquisition system (Spider 8 manufactured by HBM) was attached through electrodes at both ends of the CF sensor to simultaneously record the variation in the electrical resistance with the applied strain, which is used to calculate its gauge factor (GF). The sample was placed in the machine using paper support as it was difficult to place the CF sensor alone between the fixture of the machine and before the start of the test, the paper frame was cut in the middle to avoid any effect on the mechanical response of the CF sensor during the test, Figure 2. Also, it was vital to ensure that the CF sensor was not in contact with any metallic part of the machine because it could influence its electrical response that is why all the required parts of the machine were isolated by covering with the insulation tape. It should be kept in mind that the filaments in the CF sensor were unstrained when placed between the fixture before the test and there was no slippage between the electrode and sensor connection during the test as it was accurately and properly secured between the fixtures, Figure 3. Three successful tests were conducted with the CF sensor up to fracture to comprehend its electrical behavior with the variation in mechanical performance for high strain applications. The sensor has been subjected to tensile load at a low strain rate of 2mm/min. As one will see later, the results showed repeatability in the mechanical and electrical response of the CF sensor.

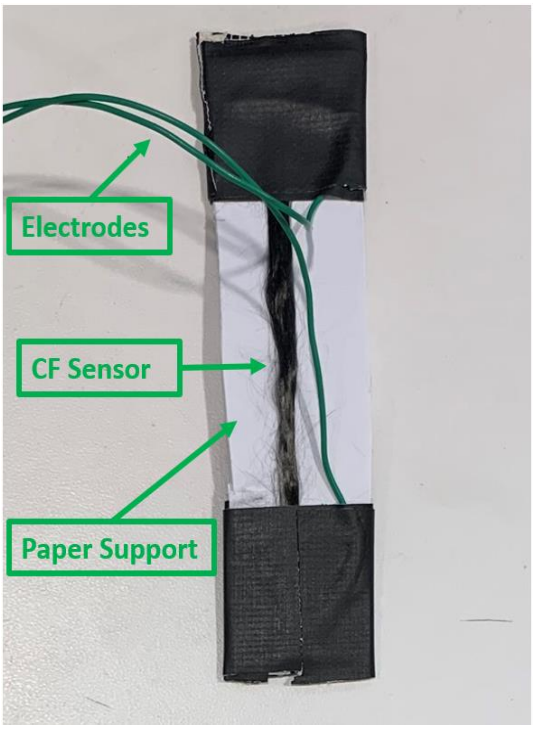

Figure 2: Preparation of CF sensor for standalone experimental test for the GF calculation. A set of papers is used as a support and the electrode is attached on each end.

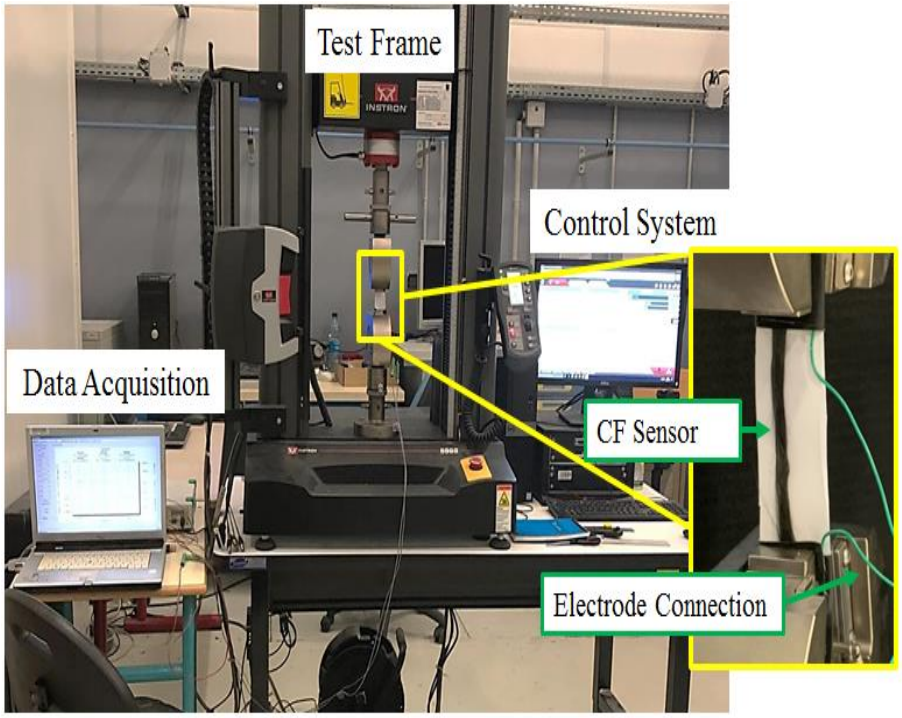

Figure 3: Experimental arrangement to examine the strain sensitivity of the CF sensor.

2.2. Experimentation of standalone CF sensor under thermal loading

CF sensor was tested under the thermal load as a standalone sensor of 72 mm in length and 5 mm width using the CECASI oven apparatus, Figure 4. The CECASI oven system has a data acquisition system in which you can design the entire program of the thermal behavior including, temperature range, each step initial and final limit, and temperature change speed from one step to another. A paper sheet was used to place all three samples in the machine to support and isolate the CF sensor from any metallic part of the shelf. The temperature of the machine was controlled using the operating system and the data acquisition system was attached to each sensor using electrodes for real-time monitoring of change in resistance with the change in temperature. A K-type thermocouple was also placed within the CECASI to verify the temperature change within the chamber. Type K thermocouple is used in this experiment. Type K is the most common type of thermocouple. Itôs inexpensive, accurate, reliable, and has a wide temperature range. The type K is commonly found in nuclear applications because of its relative radiation hardness. The maximum continuous temperature is around 1,100°C. It has a temperature range of -200°C to 1250°C with an error sensitivity of 0.4-0.75%. CECASI was programmed to change the thermal environment while thermocouple and the sensor were attached to the separate data acquisition system (Spider 8 manufactured by HBM) which can simultaneously record the thermal change of the thermocouple and resistance change of the CF sensor. The thermocouple was attached to one input of the acquisition system and electrodes attached to the sensor were attached to the other input of the acquisition system. Two sets of tests were performed on the CF sensors, the first test included increase in temperature up to 38°C starting from the room temperature i.e. 15°C and the second one included decrease in temperature up to -7°C starting from room temperature i.e 15°C. In each test, the temperature was changed by one degree with a rate of 0.2 °C/min, and at each degree, the temperature was kept constant for 10 mins. This step was carried out to understand the change in electrical resistance of the CF sensor in detail with defining the limit of precision.

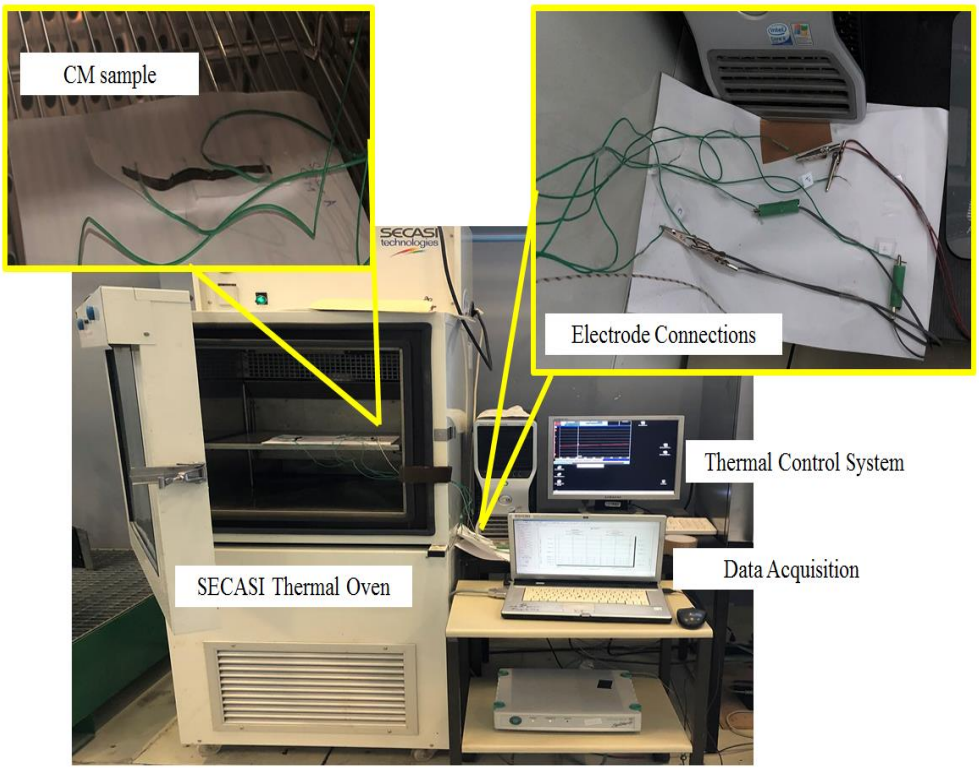

Figure 4: Experimental arrangement to examine the electrical behavior of the CM sensor under thermal loading.

3. Result discussions

3.1. Electromechanical characterization of CF sensor

The CF sensor displayed good mechanical behavior and Young's modulus and yield strength of all the examined CF sensor samples were about 94.53 MPa and 1.73 MPa on average during the standalone test, respectively, Figure 5a. Table 2 summarizes the mechanical behavior of the CF sensor, consisting of yieldôs strength, Young's modulus, and fracture strain. In overall mechanical behavior, each sensor sample exhibited linear elastic deformation before the start of the final fracture because of the high stiffness. CF sensor did not show any plastic deformation however, reduction in mechanical behavior was gradual due to the consecutive breakage of the filaments. Even though CF sensor showed high stiffness, but it was quite flexible because carbon filaments were held together loosely together and were combined only in both ends were electrodes were attached, Figure 5b. Therefore, these CF sensors showed the potential to be used in strain monitoring applications without compromising their mechanical performance. Furthermore, it was observed that the damage initiation and propagation were not sudden, and the membrane was fractured gradually with the breakage of each filament.

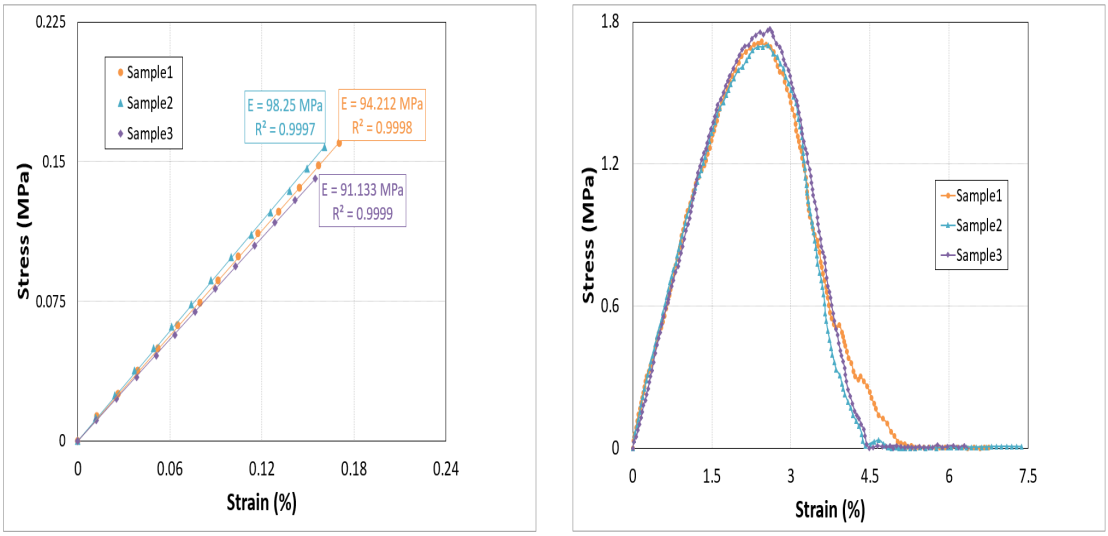

(a) Elastic Modulus *(b) Overall mechanical behavior*

Figure 5: Mechanical performance of the CF sensor.

Table 2: Mechanical properties of CF sensor under tensile loading

	Elastic Modulus (MPa)	**Fracture Strain (%)**	**Yield Strength (MPa)**
Sample 1	94.212	5.16	1.72
Sample 2	98.247	4.44	1.70
Sample 3	91.133	4.49	1.77
Average	94.53	4.46	1.73
Standard deviation	3.5677	0.0354	0.0360

The resistance of the CF sensor was increased with the applied tensile strain which verified good correlation among its electromechanical response, Figure 6a. The sensitivity of the CF sensor was demonstrated in terms of GF by comparing the variation of resistance with the amount of applied tensile strain and calculated by using equation (1).

$$G.F = \frac{\left(\Delta \frac{R}{Ro}\right)}{\varepsilon} \quad (1)$$

In this equation, $\Delta R/R_o$ is the main constituent to define the sensitivity of the CF strain sensor as it signifies the ratio of original resistance to the variation of resistance with the applied strain ε. The GF of this sensor was calculated to be inside 10.2-10.8 range within the elastic limit, Figure 6b. In

general, the GF of traditional strain sensor is around 2 while some of the multifunctional materials show higher GF values [51]. For example, E. Häntzsche et al. [52] studied the strain monitoring behavior of sensor weaved into composites in different conditions and found the GF in the range of 0.6-1.3. However, these tests were performed on the CF sensor when embedded within a glass fiber mat composites and not as a standalone sensot. So, it was confirmed from these results the CF sensor has good strain sensitivity range and might be used for instantaneous strain monitoring of structures.

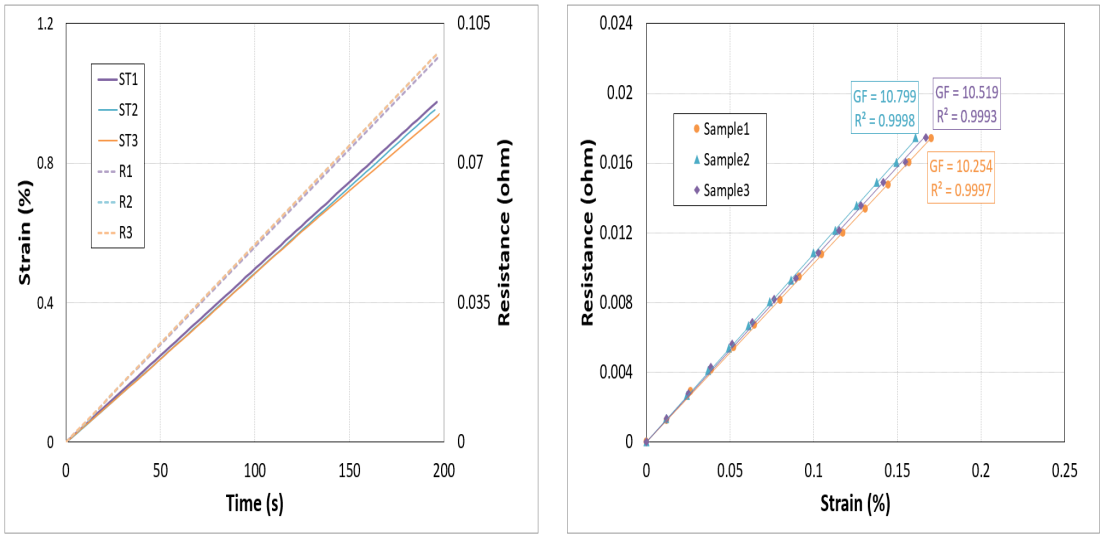

(a) Strain (ST) and Resistance (R) change *(b) GF calculation*

Figure 6: Experimental behavior and calculation of the strain sensitivity of the CF membrane sensor. ST represents the strain of all three samples and R represent the resistance of the sample.

Each specimen of the CF sensor presented good electrical behavior throughout the applied tensile strain, resistance changed gradually, and all samples displayed similar overall performance. The overall behavior of the CF sensor presented that, during elastic behavior the change in resistance was linear, and when the mechanical behavior of the sensor started to degrade there was a sudden increase in the resistance which reached maximum value upon fracture of the membrane, Figure 7. In addition, the sudden increase in the resistance of the sensor with the degradation of the mechanical behavior was progressing gradually to the maximum value because the carbon filaments in the sensor were breaking individual with the elongation, and with each breakage, the resistance showed variation. it was observed that when the strength of the CF sensor began to drop after achieving the peak value, its resistance started to increase linearly which confirmed good sensitivity of the sensor to detect damage initiation. All samples showed the same maximum stress and demonstrated the start of damage initiation at the almost same time. The degradation of stress in each sample showed the one by one failure of their filaments and this evolution or damage was slightly in comparison. This slight difference of failure was also observed in the evolution of respective electrical resistance of each sample and each CF sensor showed saturation of resistance to a maximum value when there

were complete fracture and stress reached zero value. This confirmed its ability to use for real-time strain monitoring applications during high strain deformation of structures because the sensor showed good electrical conductance until all the filaments in it were broken.

Moreover, an increase in resistance is directly proportional to an increase in the length (elongation) of the sensor, equation (2)-(3).

$$\alpha = \frac{1}{\rho} \tag{2}$$

$$R = \frac{\rho L}{A} \tag{3}$$

Where α is electrical conductivity, ρ is resistivity, L *is* length, A is the cross-sectional area, and R is resistance.

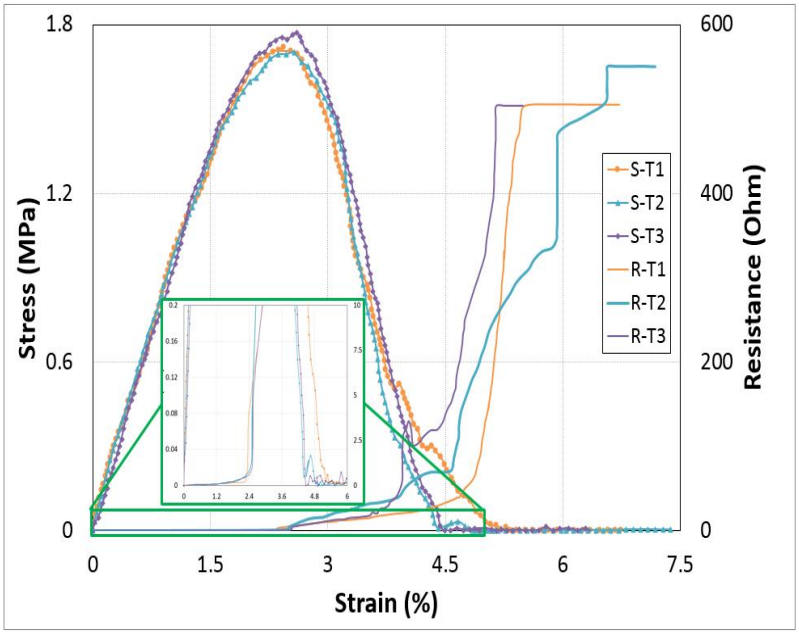

Figure 7: Overall electromechanical response of CM sensor specimens. Stress (S) response of samples in all three tests (T) is represented by S-T while Resistance (R) of samples n all three tests (T) are represented by R-T.

3.2. Electro-thermal Behavior of CF sensor

A standard two probe test was performed on three different samples between the temperature ranges of -7°C to 38°C in two sets in an oven at atmospheric pressure. Data acquisition (Spider 8 manufactured by HBM) was used to monitor the change in resistance of the CF samples and the thermocouple. A constant current of 4 mA was applied to all three samples which were randomly cut from the manufactured specimen. The applied current was kept low to prevent the self-heating of the samples and effect their electro-thermal behavior. All three samples showed an increase in resistance with an increase in temperature, Figure 8a. Moreover, each data point is provided by the error bar demonstrating the behavior of the CF sensor at each temperature change. As described earlier, the thermal load program was designed to halt the temperature change at each degree for 10 mins and

error bars show the mean distribution of these data points at each degree. The overall curve profile showed the effect of temperature on the conductivity of the sensor. It showed a nonlinear parabolic increase in the resistance with the increase in temperature. All three samples showed good reproducibility in results in both cases and small error bars ensured the precision of the readings at each change of degree. Generally, it was expected to see the opposite response with the decrease in temperature but, the CF sensor showed an almost linear increase in resistance with decreasing the temperature up to 0°C, Figure 8b. From 0°C to -7°C the resistance was increasing with the decrease in temperature, but the slope of the curve was reduced. Moreover, it was observed that there was a minute decrease in the resistance of the CF sensor with a decrease in temperature and it started to increase. The filaments were freely aligned in the center while at both ends, they were combined and attached with the electrodes using insulation tape. This means that in addition to the deformation of the carbon filaments during thermal loading, the electrical contact points also played a vital role in determining the overall electrical behavior of the sensor. During the decrease in temperature, generally, the resistance should decrease which was the case in the initial points. This decrease in resistance is because of the compression of the filaments of the sensor and this could result in the decrease in the contact points between the filaments thus, reducing the multiple paths of current flow. The change in electrical contact points could increase the resistance of the sensor, Figure 9 [53]ï [56]. This means that in addition to the deformation of the carbon filaments during thermal loading, the electrical contact points also played a vital role in determining the overall electrical behavior of the sensor. During the decrease in temperature, generally, the resistance should decrease which was the case in the initial points. This decrease in resistance is because of the compression of the filaments of the sensor and this could result in the decrease in the contact points between the filaments thus, reducing the multiple paths of current flow. The change in electrical contact points could increase the resistance of the sensor.

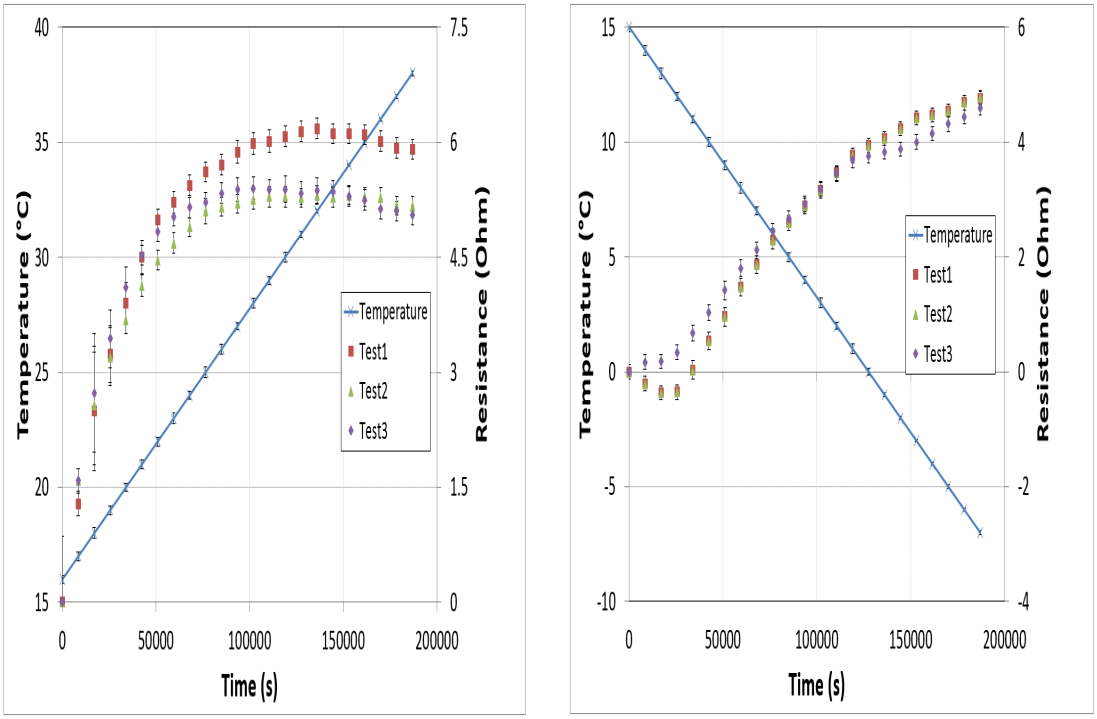

(a) Test performed with an increase in temperature

(b) Test performed with a decrease in temperature

Figure 8: Electrical behavior of CM during thermal loading to detect thermal change.

Though, it should be kept in mind that the CF sensor detected the change in the surrounding temperature by the change in its electrical behavior which could be used to detect energy release during damage failure which always results in temperature increase.

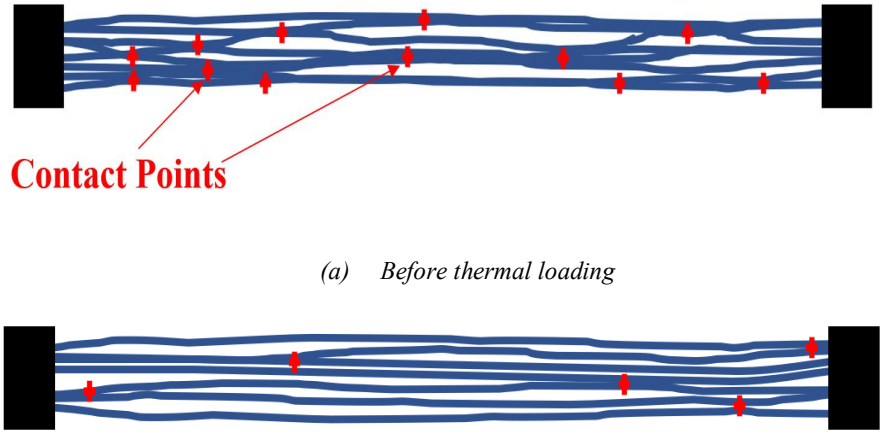

(a) Before thermal loading

(b) After thermal loading

Figure 9: Demonstration of electrical contact points between the filaments of CF sensor

To further explain the behavior of the CF sensor under thermal loading, non-linear equations were found to accurately describe the relation of the change in resistance with the change of temperature. These empirical relations were derived from the average behavior of all three samples which showed the nonlinear change in the resistance (ohm) with respect to the temperature (°C), Figure 10. Two equations were derived, one during the positive change in temperature $R(T_P)$ and one for the during the negative change in temperature $R(T_N)$. These equations are presented as follow:

$$R(T_P) = 0.0014T^3 - 0.1378T^2 + 4.3424T - 39.225 \quad (4)$$

$$R^2 = 0.9907$$

$$R(T_N) = 0.0008T^3 - 0.0158T^2 - 0.2308T + 3.9059 \quad (5)$$

$$R^2 = 0.9889$$

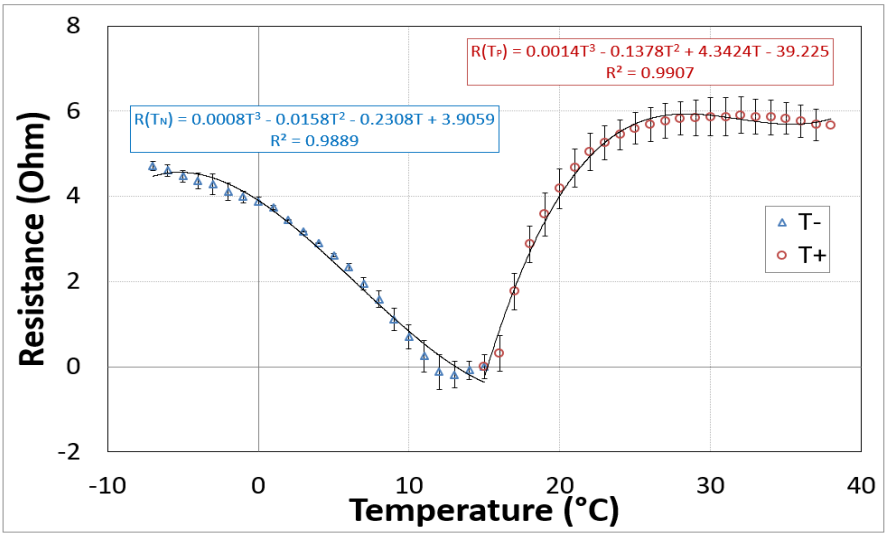

Figure 10: Calculation of empirical relations to describe the nonlinear change in resistance with respect to temperature.

Both equations represented similar empirical relations with an accuracy of 98% which further verified the behavior of sensors for the quantification of damage. The relation of resistance with time could be generalized as follow:

$$R(t) = aT^3 + bT^2 + cT^1 + d \quad (6)$$

where *a, b, c,* and *d* are empirical constants.

This change is resistance can be further related to change in length or strain induced in the sample and we can use the following relation:

$$GF = \frac{\frac{\Delta R}{R}}{\varepsilon} \quad (7)$$

$$R' = \frac{\Delta R}{R}$$

$$\varepsilon = R' * \left(\frac{1}{GF}\right) \quad (8)$$

where *GF* is the gauge factor constant of the sensor, *R* is the original resistance of the sensor, and ΔR is the change in the resistance of the sensor with the applied strain ε.

By substituting equation 6 in equation 8, the change of resistance vs. temperature can give us a change in strain vs. temperature.

$$\varepsilon(T) = R'(T) * \left(\frac{1}{GF}\right) \quad (9)$$

This equation can quantify the damage or strain rate induced in the specimen by the amount of energy released during the deformation or damage process. This can be sued to monitor damage in different structural materials in real-time.

4. Conclusions

The objective of this extensive experimental study was to develop a simple, robust, and cost-effective sensor system with high electrical conductance for multimode real-time monitoring under different loadings. This CF sensor showed viable replacement of conventional strain gauges and SHM systems because of the better flexibility, cost effectiveness, simplicity in data collection and analysis and it can be easily embedded within a sample or attached on the surface. These sensors showed high sensitivity to applied strain in the range of 10.2-10.8, were more flexible and could be easily integrated within any structure. The electro-thermal behavior showed that thermal detection with the change of resistance was because of thermal expansion and distance between the electrical connection points of straightly aligned carbon filaments in the CF sensor. Results confirmed that CF sensors in both tests reacted to the applied stimuli and showed a distinct change in their change in resistance thus, not only monitoring the deformation but also detecting the change in temperature in the surrounding at atmospheric pressure. However, further study is required to understand the precise mechanism responsible for changing the resistance of the sensors to apprehend its response under thermal loading. These CF sensors can further advance itself in real-time sensing applications within composite structures including strain monitoring, thermal degradation, and detection of failure and energy release during dynamic loading. The sensitivity of this sensor can be further tailored and

amplified as desired parameters by modifying the number and alignment of carbon filaments and without any significant requirements.

Conflict of interests: Authors have no conflict of interests

Authors statement: Y. Qureshi: Design and conduction of Experimentation, data curation, data analysis, investigation and data interpretation, writingð original draft preparation, M. Tarfaoui: supervision, writingð review and editing, project administration, and K. Lafdi: Samples preparation

References

[1] C. Simon, E. Potter, M. McCabe, and C. Baggerman, ñSmart fabrics technology development,ò 2010. [Online]. Available: https://ntrs.nasa.gov/archive/nasa/casi.ntrs.nasa.gov/20100042366.pdf.

[2] M. Tarfaoui., ñAdvances in Composite Materials-Ecodesign and Analysis.,ò InTech, 2011.

[3] A. El Moumen, M. Tarfaoui, K. Lafdi, and H.Benyahia, ñDynamic properties of carbon nanotubes reinforced carbon fibers/epoxy textile composites under low velocity impact,ò *Compos. Part B Eng.*, vol. 125, pp. 1ï 8, 2017.

[4] M. Tarfaoui, M. Nachtane, and A. El Moumen, ñEnergy dissipation of stitched and unstitched woven composite materials during dynamic compression test,ò *Compos. Part B Eng.*, vol. 167, pp. 487ï 496, 2019, doi: https://doi.org/10.1016/j.compositesb.2019.03.023.

[5] K. Diamanti and C. Soutis, ñStructural health monitoring techniques for aircraft composite structures,ò *Prog. Aerosp. Sci.*, vol. 46, no. 8, pp. 342ï 352, 2010, doi: https://doi.org/10.1016/j.paerosci.2010.05.001.

[6] O. R. Shah and M. Tarfaoui, ñDetermination of mode I & II strain energy release rates in composite foam core sandwiches: an experimental study of the composite foam core interfacial fracture resistance.,ò *Compos. Part B Eng.*, vol. 111, no. 134ï 142, 2017.

[7] S. Sassi, M. Tarfaoui, and H. Ben Yahia., ñIn-situ heat dissipation monitoring in adhesively bonded composite joints under dynamic compression loading using SHPB,ò *Compos. Part B Eng.*, vol. 54, pp. 64ï 76, 2018.

[8] Y. Qureshi, M. Tarfaoui, K. K. Lafdi, and K. Lafdi, ñDevelopment of microscale flexible nylon/Ag strain sensor wire for real-time monitoring and damage detection in composite structures subjected to three-point bend test,ò *Compos. Sci. Technol.*, vol. 181, 2019, doi: 10.1016/j.compscitech.2019.107693.

[9] J.-B. Ihn and F.-K. Chang, ñPitch-catch active sensing methods in structural health monitoring for aircraft structures,ò *Struct. Heal. Monit.*, vol. 7, no. 1, pp. 5ï 9, 2008.

[10] Y. Qureshi, M. Tarfaoui, K. K. Lafdi, and K. Lafdi, ñReal-time strain monitoring performance of flexible Nylon/Ag conductive fiber,ò *Sensors Actuators A Phys.*, vol. 295, pp. 612ï 622, 2019, doi: https://doi.org/10.1016/j.sna.2019.06.036.

[11] Y. Qureshi, M. Tarfaoui, K. K. Lafdi, and K. Lafdi, ñReal-time strain monitoring and damage detection of composites in different directions of the applied load using a microscale flexible Nylon/Ag strain sensor,ò *Struct. Heal. Monit.*, vol. 19, no. 3, pp. 885ï 901, doi: 10.1177/1475921719869986.

[12] Y. Qureshi, M. Tarfaoui, K. K. Lafdi, and K. Lafdi, ñIn-situ Monitoring, Identification and Quantification of Strain Deformation in Composites under Cyclic Flexural Loading using Nylon/Ag Fiber Sensor,ò *IEEE Sens. J.*, p. 1, 2020, doi: 10.1109/JSEN.2020.2969329.

[13] C. Bois, P. Herzog, and C. Hochard, ñMonitoring a delamination in a laminated composite beam using in-situ measurements and parametric identification,ò *J. Sound Vib.*, vol. 299, no. 4, pp. 786ï 805, 2007, doi: https://doi.org/10.1016/j.jsv.2006.07.026.

[14] V. Giurgiutiu, A. Zagrai, and J. J. Bao, ñPiezoelectric Wafer Embedded Active Sensors for Aging Aircraft Structural Health Monitoring,ò *Struct. Heal. Monit.*, vol. 1, no. 1, pp. 41ï 61, 2002, doi: 10.1177/147592170200100104.

[15] G. Park, H. H. Cudney, and D. J. Inman, ñAn Integrated Health Monitoring Technique Using Structural Impedance Sensors,ò *J. Intell. Mater. Syst. Struct.*, vol. 11, no. 6, pp. 448ï 455, 2000, doi: 10.1106/QXMV-R3GC-VXXG-W3AQ.

[16] C. C. Ciang, J.-R. Lee, and H.-J. Bang, ñStructural health monitoring for a wind turbine system: a review of damage detection methods,ò *Meas. Sci. Technol.*, vol. 19, no. 12, p. 122001, Oct. 2008, doi: 10.1088/0957-0233/19/12/122001.

[17] T. G. Gerardi, ñHealth Monitoring Aircraft,ò *J. Intell. Mater. Syst. Struct.*, vol. 1, no. 3, pp. 375ï 385, 1990, doi: 10.1177/1045389X9000100307.

[18] C. R. Farrar and K. Worden, ñAn introduction to structural health monitoring,ò *Philos. Trans. R. Soc. A Math. Phys. Eng. Sci.*, vol. 365, no. 1851, pp. 303ï 315, 2007, doi: 10.1098/rsta.2006.1928.

[19] J. Leng and A. Asundi, ñStructural health monitoring of smart composite materials by using EFPI and FBG sensors,ò *Sensors Actuators A Phys.*, vol. 103, no. 3, pp. 330ï 340, 2003, doi: https://doi.org/10.1016/S0924-4247(02)00429-6.

[20] W. Staszewski, C. Boller, and G. R. Tomlinson, *Health monitoring of aerospace structures: smart sensor technologies and signal processing*. John Wiley & Sons, 2004.

[21] Y. ZOU, L. TONG, and G. P. STEVEN, ñVIBRATION-BASED MODEL-DEPENDENT DAMAGE (DELAMINATION) IDENTIFICATION AND HEALTH MONITORING FOR COMPOSITE STRUCTURES ð A REVIEW,ò *J. Sound Vib.*, vol. 230, no. 2, pp. 357ï 378, 2000, doi: https://doi.org/10.1006/jsvi.1999.2624.

[22] A. C. Raghavan and C. Cesnik, ñReview of Guided-Wave Structural Health Monitoring,ò *Shock Vib. Dig.*, vol. 39, pp. 91ï 114, 2007, doi: 10.1177/0583102406075428.

[23] S. W. Doebling, C. R. Farrar, M. B. Prime, and D. W. Shevitz, ñDamage identification and health monitoring of structural and mechanical systems from changes in their vibration characteristics: A literature review,ò doi: 10.2172/249299.

[24] J. P. Andrews, A. N. Palazotto, M. P. DeSimio, and S. E. Olson, ñLamb Wave Propagation in Varying Isothermal Environments,ò *Struct. Heal. Monit.*, vol. 7, no. 3, pp. 265ï 270, 2008, doi: 10.1177/1475921708090564.

[25] R. Schueler, S. P. Joshi, and K. Schulte, ñDamage detection in CFRP by electrical conductivity mapping,ò *Compos. Sci. Technol.*, vol. 61, no. 6, pp. 921ï 930, 2001, doi: https://doi.org/10.1016/S0266-3538(00)00178-0.

[26] A. Kunadt, E. Starke, G. Pfeifer, and C. Cherif, ñMesstechnische Eigenschaften von Dehnungssensoren aus Kohlenstoff-Filamentgarn in einem VerbundwerkstoffMeasuring

Performance of Carbon Filament Yarn Strain Sensors Embedded in a Composite,ò *tm-Technisches Mess. Plattf. für Methoden, Syst. und Anwendungen der Messtechnik*, vol. 77, no. 2, pp. 113ï 120, 2010.

[27] H. C. H. Li, I. Herszberg, C. E. Davis, A. P. Mouritz, and S. C. Galea, ñHealth monitoring of marine composite structural joints using fibre optic sensors,ò *Compos. Struct.*, vol. 75, no. 1, pp. 321ï 327, 2006, doi: https://doi.org/10.1016/j.compstruct.2006.04.054.

[28] J. Rausch and E. Mäder, ñHealth monitoring in continuous glass fibre reinforced thermoplastics: Tailored sensitivity and cyclic loading of CNT-based interphase sensors,ò *Compos. Sci. Technol.*, vol. 70, no. 13, pp. 2023ï 2030, 2010, doi: https://doi.org/10.1016/j.compscitech.2010.08.003.

[29] M. M. B. Hasan, A. Matthes, P. Schneider, and C. Cherif, ñApplication of carbon filament (CF) for structural health monitoring of textile reinforced thermoplastic composites,ò *Mater. Technol.*, vol. 26, no. 3, pp. 128ï 134, 2011, doi: 10.1179/175355511X13007211258881.

[30] J. Rausch and E. Mäder, ñHealth monitoring in continuous glass fibre reinforced thermoplastics: Manufacturing and application of interphase sensors based on carbon nanotubes,ò *Compos. Sci. Technol.*, vol. 70, no. 11, pp. 1589ï 1596, 2010, doi: https://doi.org/10.1016/j.compscitech.2010.05.018.

[31] J. Rausch and E. Mäder, ñCarbon nanotube coated glass fibres for interphase health monitoring in textile composites,ò *Mater. Technol.*, vol. 26, no. 3, pp. 153ï 158, 2011, doi: 10.1179/175355511X13007211259042.

[32] N. Forintos and T. Czigany, ñReinforcing carbon fibers as sensors: The effect of temperature and humidity,ò *Compos. Part A Appl. Sci. Manuf.*, vol. 131, p. 105819, 2020, doi: https://doi.org/10.1016/j.compositesa.2020.105819.

[33] S. Park *et al.*, ñStretchable Energy-Harvesting Tactile Electronic Skin Capable of Differentiating Multiple Mechanical Stimuli Modes,ò *Adv. Mater.*, vol. 26, no. 43, pp. 7324ï 7332, Nov. 2014, doi: 10.1002/adma.201402574.

[34] M. Boehle, Q. Jiang, L. Li, A. Lagounov, and K. Lafdi, ñCarbon nanotubes grown on glass fiber as a strain sensor for real time structural health monitoring,ò *Int. J. Smart Nano Mater.*, vol. 3, no. 2, pp. 162ï 168, Jun. 2012, doi: 10.1080/19475411.2011.651509.

[35] S. Y. Kim, S. Park, H. W. Park, D. H. Park, Y. Jeong, and D. H. Kim, ñHighly Sensitive and Multimodal All-Carbon Skin Sensors Capable of Simultaneously Detecting Tactile and Biological Stimuli,ò *Adv. Mater.*, vol. 27, no. 28, pp. 4178ï 4185, Jul. 2015, doi: 10.1002/adma.201501408.

[36] C. Pang *et al.*, ñA flexible and highly sensitive strain-gauge sensor using reversible interlocking of nanofibres,ò *Nat. Mater.*, vol. 11, no. 9, pp. 795ï 801, 2012, doi: 10.1038/nmat3380.

[37] I. Krucinska and T. Stypka, ñDirect measurement of the axial poissonôs ratio of single carbon fibres,ò *Compos. Sci. Technol.*, vol. 41, no. 1, pp. 1ï 12, 1991, doi: https://doi.org/10.1016/0266-3538(91)90049-U.

[38] S. Blazewicz, B. Patalita, and P. Touzain, ñStudy of piezoresistance effect in carbon fibers,ò *Carbon N. Y.*, vol. 35, no. 10, pp. 1613ï 1618, 1997, doi: https://doi.org/10.1016/S0008-6223(97)00120-6.

[39] C. N. Owston, ñElectrical properties of single carbon fibres,ò *J. Phys. D. Appl. Phys.*, vol. 3, no. 11, pp. 1615ï 1626, Nov. 1970, doi: 10.1088/0022-3727/3/11/309.

[40] A. Horoschenkoff, T. Mueller, and A. Kroell, ñOn the characterization of the piezoresistivity of embedded carbon fibres,ò *ICCM 17th*, 2009.

[41] A. Horoschenkoff, M. Derks, T. Mueller, H. Rapp, and S. Schwarz, ñKonzeptstudie zum einsatz von elektrisch kontaktierten carbonfasern als sensor für leichtbaustrukturen aus faserverbundwerkstoff Vorträge. 14,ò in *Nationales Symp. Sampe Deutschland eV (Garching, 7--28 February)*, 2008.

[42] P. C. CONOR and C. N. OWSTON, ñElectrical Resistance of Single Carbon Fibres,ò *Nature*, vol. 223, no. 5211, pp. 1146ï 1147, 1969, doi: 10.1038/2231146b0.

[43] J. Wen, Z. Xia, and F. Choy, ñDamage detection of carbon fiber reinforced polymer composites via electrical resistance measurement,ò *Compos. Part B Eng.*, vol. 42, no. 1, pp. 77ï 86, 2011, doi: https://doi.org/10.1016/j.compositesb.2010.08.005.

[44] C. Luan, X. Yao, H. Shen, and J. Fu, ñSelf-Sensing of Position-Related Loads in Continuous Carbon Fibers-Embedded 3D-Printed Polymer Structures Using Electrical Resistance Measurement,ò *Sensors (Basel).*, vol. 18, no. 4, p. 994, Mar. 2018, doi: 10.3390/s18040994.

[45] X. Yao, C. Luan, D. Zhang, L. Lan, and J. Fu, ñEvaluation of carbon fiber-embedded 3D printed structures for strengthening and structural-health monitoring,ò *Mater. Des.*, vol. 114, pp. 424ï 432, 2017, doi: https://doi.org/10.1016/j.matdes.2016.10.078.

[46] Y. Goldfeld, S. Ben-Aarosh, O. Rabinovitch, T. Quadflieg, and T. Gries, ñIntegrated self-monitoring of carbon based textile reinforced concrete beams under repeated loading in the un-cracked region,ò *Carbon N. Y.*, vol. 98, pp. 238ï 249, 2016, doi: https://doi.org/10.1016/j.carbon.2015.10.056.

[47] F.-Y. Yeh, K.-C. Chang, and W.-C. Liao, ñExperimental Investigation of Self-Sensing Carbon Fiber Reinforced Cementitious Composite for Strain Measurement of an RC Portal Frame,ò *Int. J. Distrib. Sens. Networks*, vol. 11, no. 11, p. 531069, 2015, doi: 10.1155/2015/531069.

[48] A. Todoroki, Y. Samejima, Y. Hirano, and R. Matsuzaki, ñPiezoresistivity of unidirectional carbon/epoxy composites for multiaxial loading,ò *Compos. Sci. Technol.*, vol. 69, no. 11, pp. 1841ï 1846, 2009, doi: https://doi.org/10.1016/j.compscitech.2009.03.023.

[49] N. Angelidis, C. Y. Wei, and P. E. Irving, ñThe electrical resistance response of continuous carbon fibre composite laminates to mechanical strain,ò *Compos. Part A Appl. Sci. Manuf.*, vol. 35, no. 10, pp. 1135ï 1147, 2004, doi: https://doi.org/10.1016/j.compositesa.2004.03.020.

[50] J. B. Park, T. Okabe, N. Takeda, and W. A. Curtin, ñElectromechanical modeling of unidirectional CFRP composites under tensile loading condition,ò *Compos. Part A Appl. Sci. Manuf.*, vol. 33, no. 2, pp. 267ï 275, 2002, doi: https://doi.org/10.1016/S1359-835X(01)00097-5.

[51] ñStrain Gauge Measurement ï A Tutorial,ò 1998. [Online]. Available: http://elektron.pol.lublin.pl/elekp/ap_notes/NI_AN078_Strain_Gauge_Meas.pdf.

[52] E. Häntzsche, A. Matthes, A. Nocke, and C. Cherif, ñCharacteristics of carbon fiber based strain sensors for structural-health monitoring of textile-reinforced thermoplastic composites depending on the textile technological integration process,ò *Sensors Actuators A Phys.*, vol. 203, pp. 189ï 203, 2013, doi: https://doi.org/10.1016/j.sna.2013.08.045.

[53] D.-J. Kwon, P.-S. Shin, J.-H. Kim, Z.-J. Wang, K. L. DeVries, and J.-M. Park, ñDetection of damage in cylindrical parts of carbon fiber/epoxy composites using electrical resistance (ER) measurements,ò *Compos. Part B Eng.*, vol. 99, pp. 528ï 532, 2016, doi: https://doi.org/10.1016/j.compositesb.2016.06.050.

[54] D.-J. Kwon, Z.-J. Wang, J.-Y. Choi, P.-S. Shin, K. L. Devries, and J. M. Park, ñInterfacial evaluation of carbon fiber/epoxy composites using electrical resistance measurements at room and a cryogenic temperature,ò *Compos. Part A Appl. Sci. Manuf.*, vol. 72, 2015, doi: 10.1016/j.compositesa.2015.02.007.

[55] Z. Wang, L. Ye, and Y. Liu, ñElectro-thermal damage of carbon fiber/epoxy composite laminate,ò *J. Reinf. Plast. Compos.*, vol. 37, no. 3, pp. 166ï 180, 2018, doi: 10.1177/0731684417738334.

[56] H. Yu, D. Heider, and S. Advani, ñPrediction of effective through-thickness thermal conductivity of woven fabric reinforced composites with embedded particles,ò *Compos. Struct.*, vol. 127, pp. 132ï 140, 2015, doi: https://doi.org/10.1016/j.compstruct.2015.03.015.